Carbohydrate Polymers 84 (2011) 1093–1102

Contents lists available at ScienceDirect

Carbohydrate Polymers

journal homepage: www.elsevier.com/locate/carbpol

Nanofibers based on polysaccharides from the green seaweed *Ulva Rigida*

Georgios Toskas[a,*], Rolf-Dieter Hund[a], Ezzedine Laourine[a], Chokri Cherif[a], Vangelis Smyrniotopoulos[b], Vassilios Roussis[b]

[a] Institute of Textile Machinery and High Performance Material Technology (ITM), Technische Universität Dresden, Hohestr. 6, 01069 Dresden, Germany
[b] University of Athens, School of Pharmacy, Department of Pharmacognosy and Chemistry of Natural Products, Panepistimiopolis Zografou, Athens 15771, Greece

ARTICLE INFO

Article history:
Received 13 October 2010
Received in revised form
23 December 2010
Accepted 23 December 2010
Available online 8 January 2011

Keywords:
Polysaccharide ulvan
Nanofibers
Electrospinning
Ulvan/poly(vinyl alcohol) fibers
Crystallinity
Biomaterial

ABSTRACT

The nanofiber ability of an ulvan-rich extract, originated from the low cost biomass of the alga *Ulva rigida*, has been achieved for the first time via electrospinning. Ulvan-based uniform nanofibers were produced by being blended with poly(vinyl alcohol) (PVA). The nanofibers have an average diameter controllable down to 84 nm and present a highly ordered crystalline structure under transmission electron microscopy (TEM). A new complex fiber is created, which results from ulvan-rich extract and PVA ionic assembly and involves borate esters and divalent cations. The spinnability of this anionic sulfated polysaccharide-rich extract in combination with its interesting biological and physicochemical properties can lead to new biomedical applications such as drug release systems.

1. Introduction

Nanofiber matrices originated from natural polymers have gotten increasing attention for their application in the biomedical sector, e.g. tissue engineering scaffolds, wound dressing and drug delivery (Greiner & Wendorf, 2007; Lee, Jeong, Kang, Lee, & Park, 2009; Venugopal & Ramakrishna, 2005). Natural polymers possess proven tissue compatibility and usually contain domains that can send important signals to guide cells at various stages of their development. The most used sources of natural derived polymers include proteins, especially from extracellular matrices (ECM) (e.g. collagen), polypeptides, polysaccharides (including chitosan, starch, hyaluronic acid and alginate) and poly(hydroxyalkanoates) (Jagur-Grodzinski, 2006; Mano & Reis, 2007). Polysaccharides of animal origin (e.g. heparin and hyaluronic acid) can raise the concern of immunogenicity and the risk of disease transmission by host organisms (Stevens, 2008) in contrary to polysaccharides of plant origin (e.g. cellulose and starch) or marine algal origin (e.g. alginate and ulvan).

Ulvan is a complex acidic sulfated polysaccharide extracted from the cell-walls of the green sea weed Ulvales (Chlorophyta). The generated and underexploited biomass from proliferating algae in eutrophicated coastal waters represents a low cost source of great potential in renewable polymers such as ulvan. The structure and the composition of ulvan has been the topic of intensive investigations by Lahaye et al. (Lahaye & Robic, 2007; Lahaye, 1998; Quemener, Lahaye, & Bobin Dubigeon, 1997; Robic, Gaillard, Sassi, Lerat, & Lahaye, 2009; Robic, Rondeau-Mouro, Sassi, Lerat, & Lahaye, 2009). Sulfate, rhamnose, xylose, glucuronic and iduronic acids are the main constituents of ulvan. In general, the main disaccharide units that constitute the aldobiuronic acid blocks of ulvan, also reported as ulvanobiuronic acid 3-sulfate (Paradossi, Cavalieri, & Chiessi, 2002; Robic, Gaillard, et al., 2009), are formed by a Type A_{3s} glucuronorhamnose and a Type B_{3s} iduronorhamnose, arranged in regular sequences within the heteropolymer chain (Fig. 1). This chemical composition could, analogously to mammalian glycosaminoglycans (GAGs), provide this yet greatly unexplored polysaccharide with antithrombogenic properties such as that of heparin (Chupa, Foster, Sumner, Madihally, & Matthew, 2000). Interestingly enough, ulvan has shown several physicochemical and biological properties (Lahaye & Robic, 2007) that could have a potential impact in many applications. It has been reported as anticoagulant (Zhang et al., 2008), antioxidant (Morelli & Chiellini, 2010; Qi et al., 2006), antitumor and immune modulator (Kaeffer, Benard, Lahaye, Blottiere, & Cherbut, 1999), lowering the low-density lipoprotein cholesterol (LDL-cholesterol), thus reducing the atherogenic index (Yu et al., 2003), and binding heavy metals (Lahaye & Robic, 2007; Webster, Murphy, Chudek, & Gadd, 1997). Ulvan belongs to the dietary fibers of "sea lettuce" which is not degraded by human endogenous enzymes and *Ulva rigida* has been

* Corresponding author. Tel.: +49 351 46342244; fax: +49 351 4634026.
E-mail address: Georgios.Toskas@tu-dresden.de (G. Toskas).

0144-8617/$ – see front matter © 2011 Elsevier Ltd. All rights reserved.
doi:10.1016/j.carbpol.2010.12.075

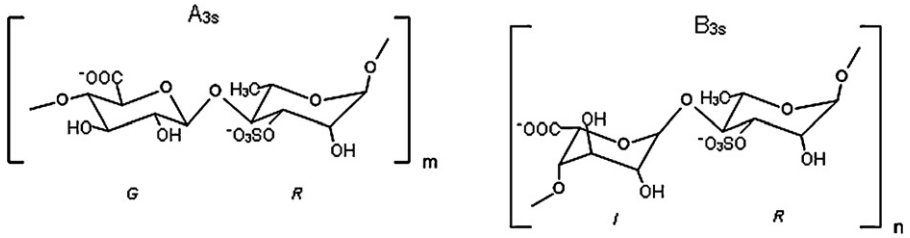

Fig. 1. The structure of the main disaccharide units in *Ulva* ulvan: A_{3s} consisting of [β-DGlcp A-(1,4)-α-L-Rhap 3s] and B_{3s} consisting of [α-L-Idop A-(1,4)-α-L-Rhap 3s]; G: (1,4)-linked β-D-glucuronic acid; R: (1,4)-linked α-L-rhamnose-3-sulfate; I: (1,4)-linked α-L-iduronic acid.

found to contain high amounts of good-quality protein, carbohydrates, vitamins and minerals (Taboada, Millán, & Míguez, 2010).

Despite the fact that ulvan has been considered a dietary fiber for a long time (Lahaye & Kaeffer, 1997), no attempt known to the author has been made to produce fibers with ulvan. Only raw micronized fibers, as evaluated by screening with ASTM sieves (Chiellini, Cinelli, Ilieva, & Martera, 2008), or raw lyophilized elongated filaments (Robic, Gaillard, et al., 2009) observed by SEM have already been reported about. Electrospun nonwoven fibrous materials of several natural polymers have been synthesized and characterized with respect to their application as biocompatible or bioresorbable materials (Jiang, Fang, Hsiao, Chu, & Chen, 2004; Toskas, Laourine, Kaeosombon, & Cherif, 2009). Typically electrospun polysaccharides are chitin, chitosan, hyaluronic acid, cellulose/cellulose derivatives and more recently alginate (Lee et al., 2009). One of the most difficult constraints to overcome for a successful electrospinning is the limited solubility of several polysaccharides. This issue can be overcome by varying the blend ratio with other polymers and by varying the solvent composition. In electrospinning, the polymers for blending used most are poly(ethylene oxide) (PEO) and poly(vinyl alcohol) (PVA). PVA as well as PEO are biocompatible polymers and are among the few synthetic polymers approved for internal use in cosmetics, personal care products and pharmaceuticals. As most polysaccharides, ulvan shows a complex solution-gelling behavior and a non-typical solvation in water resulting in a micro-aggregating gel. It is giving thermoreversible gels (Haug, 1976; Lahaye & Axelos, 1993) controlled by counter ions (cations), polymer concentration and pH (Lahaye & Robic, 2007; Robic, Gaillard, et al., 2009) under specific conditions.

In this study, the spinnability of ulvan-rich extracted polysaccharides (referred to as ulvan in this paper, for simplicity) from the green seaweed species *U. rigida* was examined and attempts to electrospin the pure ulvan-rich extract were performed with concentrations of 1.6% (w/v) up to 6.4% (w/v) by varying the solvent system. Co-blending polymers were used to reduce the viscosity of ulvan solutions so that the solution is spinnable at higher polymer concentrations. Efforts made with PEO had only partial success giving a beaded net. Conversely, defect free nanofibers were fabricated by electrospinning ulvan/PVA solutions with appropriate ulvan-to-PVA mass ratios and polymer concentrations.

2. Experimental

2.1. Material

2.1.1. Plant material

U. rigida was collected in Chalkida, Greece, at a depth of 0.5–1 m in March 2008. The seaweeds were cleaned from epiphytes, rinsed with seawater and tap-water, and dried in continuous air flow. The dried alga was then cut in 1–5 mm pieces with a mill and stored until use in plastic bags in a dry, dark place at room temperature. A specimen is kept at the Herbarium of the Laboratory of Pharmacognosy and Chemistry of Natural Products, University of Athens (ATPH/MO/205).

2.1.2. Extraction

In order to extract the ulvan polysaccharides, 100 g of the air-dried alga was suspended in 2000 mL of water and autoclaved at 130 °C for 30 min. The hot aqueous solution was separated by successive filtration through gauze and siliceous earth as filter aids and the biomass was then discarded. Afterwards, the solution was concentrated in about 1000 mL under reduced pressure and dialyzed for 48 h. The polysaccharides were precipitated by the addition of 4000 mL of 95% (v/v) ethanol. The resultant precipitate was washed three times with dry ethanol, and then dried at 80 °C (mean yield, 24.3%).

2.1.3. Chemical analysis

Protein content was determined by the micro-Kjeldahl method (N × 6.25). Ash was determined gravimetrically after incineration of samples at 550 °C for 16 h followed by 2 h at 900 °C. Total sugar content of the extracts was determined colorimetrically by the phenol–sulphuric method, with glucose as standard (Dubois, Gilles, Hamilton, Rebers, & Smith, 1956). The uronic acid content was determined by the *m*-hydroxydiphenyl method, with glucuronic acid as standard (Blumenkrantz & Asboe-Hansen, 1973). Neutral sugars were determined after hydrolysis for 3 h at 120 °C in 2 N trifluoroacetic acid (Quemener & Thibault, 1990). Monosaccharides were analysed by gas chromatography–mass spectrometry after conversion of the hydrolysate into alditol acetates following a previously described method (Sassaki et al., 2008). The alditol acetates obtained were analysed in a FOCUS-DSQ gas chromatography–mass spectrometry system operating in Electron Impact ionisation mode at 70 eV, equipped with a split–splitless injector. Injection was performed at 220 °C in a split ratio 1:10, while detection was performed at 280 °C. The column employed for the analysis was a HP-5 MS fused silica capillary column (30 m × 0.25 mm; film thickness 0.25 μm). The carrier gas was helium at a flow rate of 1.5 mL/min. The oven temperature was 60 °C at the time of the injection, raised to 300 °C at a rate of 3 °C/min and subsequently held at 300 °C for 10 min. The sulfate content of the polysaccharide extract was measured according to Kawai, Seno, and Anno (1969).

2.1.4. Gel-permeation chromatography (GPC) analysis

The molecular weight distribution of *U. rigida* polysaccharide was determined by high performance size exclusion chromatography (HPSEC) coupled to an ultraviolet (UV) and RI detection (HPSEC–UV–RI) system. The HPSEC–UV–RI system consisted of a pump (LC-20AD, Shimadzu), an auto-sampler injector (SIL-20A Prominence Shimadzu), a SEC column (250 cm × 9.4 mm ID, ZORBAX GF-250; Agilent Technologies, Canada), a UV detector at 280 nm (Waters 486) and a differential refractive index detector (RID-10A, Shimadzu). The column was maintained at 40 °C and the mobile phase was 0.7% (w/v) Na_2SO_4 at a rate of 0.5 mL/min. The

lyophilized samples (5 mg) were dissolved in 0.7% (w/v) sodium sulfate (1 mL), heated for 1 min at 90 °C and filtered through 0.4 μm filter membrane before analysis. The injection volume of the samples was 100 μL.

Column calibration was performed with glucose and standard pullulans (M_w: 5.9, 11.8, 22.8, 47.3, 112.0, 212.0, 404.0 and 788 kDa, respectively) and the calibration curve was obtained by the following sigmoid equation using Sigma Plot 10.0 software: $T = 13.633 + 14.4126/1 + e^{\ln M - 9.8443/1.1948}$ ($R^2 = 0.9992$), where M is the molecular weight of samples and T the eluting time of samples in HPSEC analysis.

2.1.5. Infrared spectroscopy

IR spectra in Fig. 6A–D were obtained using the attenuated total reflection (ATR) method on a FTIR Bruker Tensor 27 spectrophotometer. The IR spectra of electrospun ulvan/PVA (70:30) (E) and 12% PVA solution (F) were recorded using a Nicolet 210 spectrometer equipped with Omnic ESP.5.2 software.

2.1.6. NMR spectroscopy

NMR spectra were recorded using a Bruker DRX 400 spectrometer. 10 mg samples were deuterium-exchanged in 99.9% D_2O before the solubilization in 0.5 mL 100% D_2O. Chemical shifts are given on a δ (ppm) scale using TMS as the internal standard.

2.1.7. Other material

The poly(vinyl alcohol) (PVA) used in these experiments had two provenances: Sloviol® R was purchased from Novacke, Slovakia (M_W = 60,000 Da) and PVA with an average M_w = 31,000–50,000 Da (98–99% hydrolyzed) from Aldrich. Poly(ethylene oxide) (PEO) (M_W = 900,000 Da), boric acid and calcium chloride were purchased from Sigma, Germany. Acetic acid and other solvent media were purchased from Merck, Germany. Deionized water was used for the solvent systems.

2.2. Electrospinning conditions

The electrospinning apparatus was set up horizontally and the spinneret was mounted on an electrically insulated chamber. An in-house fabricated high-voltage DC power supply generator allowed voltages of up to 50 kV. The polymer solution was put into a 1 mL disposable syringe fitted with 0.60–1.0 mm 23 gauge tip-ground-to-flat needles and fed with the help of a programmable KD scientific pump. The nanofibers were collected horizontally on a polypropylene non-woven fabric or aluminum foil fitted on a stable circular collector of 12 cm diameter at different distances from 5 to 15 cm. The electric potential, solution flow rates and the needle to collector distance were adjusted so that a stable jet was obtained. The flow rate is dependent on the viscosity of the solutions and had to be adjusted with the electric field. The ambient conditions occurred at temperatures of 20–22 °C and 26–33% RH. Typical parameters operated in this study were flow rates between 0.04 and 0.10 mL/h, voltages between 28 and 30 kV and a tip to collector optimal distance of 12 cm.

2.3. Preparation of solutions for electrospinning

A solution containing 15 mM H_3BO_3 and 7 mM $CaCl_2$ in a ratio of 60/40 (v/v) was prepared in deionized water. Solutions for ulvan were adjusted at 2.34 wt% of ulvan in this medium. The solutions were stirred on a magnetic stir plate for at least 6 h until the formation of a uniform gel. A 12 wt% PVA water solution was prepared separately and stirred for a period of 24–48 h. 3 wt% PEO was also prepared either in water or in 0.5 M acetic acid. Then, the ulvan and PVA (or PEO) solutions of different proportions were mixed in various ratios of ulvan to PVA ranging from 50/50 to 90/10, and the resultant mixtures were stirred for 4 h to ensure adequate mixing. All solutions were centrifuged to remove the bubbles before being electrospun.

Table 1
Chemical composition (mol%) of the polysaccharide extract (ulvan) from *Ulva rigida*.

Rha	Xyl	Man	Ara	Gal	Glc	Uronic acids	$SO_4^{=}$
25.4	4.3	1.4	0.8	1.2	6.8	18.7	41.4

2.4. Characterization

2.4.1. Rheology

A Haake MARS (Haake, Germany) stress-controlled rheometer was used for the measurements of the solutions viscosity parameters. A 20 mm radius parallel plate (Ti) was used for the shear measurements and a cone-plate geometry (35 mm radius, 2°, Ti) for the oscillatory movement. The gap for all solutions was 0.100 mm at a temperature of 20 ± 0.1 °C.

2.4.2. Microscopy: scanning electron microscopy, transmission electron microscopy

A DSM 982 Gemini (Zeiss, Germany) scanning electron microscope served for the examination of the morphology of the nanofibers. The as-spun nanofibers were dried under vacuum at room temperature and sputter-coated with silver/graphite. The samples were examined at an accelerating voltage of 1.0 kV and magnifications from 1000 to 50,000. The SEM images were then used to evaluate the fiber diameter. The average fiber diameter was determined using Scion Imaging software in conjunction with the SEM image. Ten different fiber diameters were determined and averaged to find the fiber diameter reported for each of the resulting electrospun mats. The 95% confidence limits of the mean were calculated and reported with each average fiber diameter.

High-resolution transmission electron microscopy (HRTEM) was used to determine the morphology of nanofiber. Nanofibers for TEM were directly deposited onto a conductive carbon fabric. For sample preparation, 200 mesh copper grids containing a graphite membrane of 20 nm thickness (Plano) are used. TEM analysis was performed on a Phillips CM200 electron microscope with CS correction.

3. Results and discussion

3.1. Components of the ulvan-rich polysaccharide extract

Hot water extraction of the dried alga *U. rigida* allowed for the recovery of 24.3% polysaccharide extract. Analysis by gel permeation chromatography revealed that the acidic polysaccharides had a molecular weight distribution from 30,580 to 59,950 Da. Chemical analysis revealed that the extract used in the present study is composed of 39.8% carbohydrates, 15.5% sulfate, 0.2% protein and 24.6% ash on a dry weight basis. The main sugars of the acidic sulfated polysaccharides were rhamnose (mol.%, 25.4) and uronic acids (mol.%, 18.7) as shown in Table 1. The structures of the acidic polysaccharides were supported by infrared spectroscopy. The infrared absorption spectrum of ulvan-rich extract from *U. rigida* is shown in Fig. 6. All characteristic absorbances typical for ulvan polysaccharides, were observed (Lahaye & Ray, 1996; Lahaye, Brunel, & Bonnin, 1997; Lahaye, Inizan, & Vigouroux, 1998; Lahaye et al., 1999; Mao, Zang, Li, & Zhang, 2006; Paradossi, Cavalieri, Pizzoferrato, & Liquori, 1999; Pengzhan et al., 2003; Qi et al., 2005; Ray & Lahaye, 1995; Robic, Bertrand, Sassi, Lerat, & Lahaye, 2009). Briefly, the signal at 1620 cm^{-1} can be attributed to the asymmetrical stretching of the uronic acid carboxylate groups and the maximum absorption at 1050 cm^{-1} can be attributed to the C–O

stretching of the two main glucosides, rhamnose and glucuronic acid (Pengzhan et al., 2003; Robic, Gaillard, et al., 2009). A strong O–H stretching mode is also centered at 3340 cm^{-1}. The carboxylate groups are showing a second, weaker symmetric stretching at 1420 cm^{-1}. The observed absorption at 1240 cm^{-1} shows the presence of sulfate ester substitution of rhamnoses, while the two bands at 845 and 785 cm^{-1} are not certainly indicative of the axial O-2 position sulfate esters but they are related to the sugar cycles (Ray & Lahaye, 1995). The polysaccharide extract was also analysed by ^1H NMR spectroscopy. Typical ulvan proton chemical shifts were observed (Electronic Supplementary Information (ESI), SF. 1). In the spectra, the signals for the ulvanobiuronic acid 3-sulfate type A and B were observed. Peak attributions were recorded during comparisons with published data for ulvan and ulvan oligosaccharides (Lahaye & Ray, 1996; Lahaye et al., 1997, 1998, 1999).

3.2. Properties of solutions

Although electrospinning is generally considered the easiest method for obtaining nanofibers, its applicability to a new material such as this complex polysaccharide of ulvan is not straightforward. Several engineering and mainly physico-chemical parameters such as viscosity and polymer concentration have to be examined at once. The highly charged jet emitted from the anode (needle tip) must enhance a whipping mode in order to deposit and neutralize at the cathode (collector) with simultaneous rapid evaporation of the solvent (Reneker, Yarin, Fong, & Koombhongse, 2000). Thus, the solvent performs a crucial role in electrospinning, as inherent solvent parameters such as surface tension, dielectric constant and vapor pressure are having an important impact on the polymer solvation and subsequent bending instability. In the electrospinning of any aqueous solution, the high surface tension of water (72.8 mN/m at 20 °C) demands stronger electric fields and thus higher voltages.

In an attempt to improve the ulvan solubility and examine an easier eventual fiber formation, different solvent systems with lower dielectric constant and surface tension have been tested. Acetone up to 50% has been unsuccessful for the dissolution and gel formation of ulvan up to 6.4% (w/v), when added in the beginning. When a strongly gelled ulvan of 3.2% (w/v) was diluted up to 50% with acetone, a clearer yellowish bubbling solution was obtained, indicative of a reaction, which did not result in electrospinning. The use of dichloromethane (CH_2Cl_2) was also revealed as unsuccessful to providing appropriate solutions. The addition of up to 60% of dimethyl sulfoxide (DMSO) had better results for the solution homogeneity. Yet, electrospinning attempts resulted in droplet formations or electrospraying. After various trial combinations with negative spinning results, the solvent system of boric acid and calcium was concentrated on.

It is known (Graessley, 1980) that at low polymer concentration, below a critical chain entanglement concentration c_e, the solution does not contain sufficient overlapped polymer chains to produce uniform nanofibers. It has also been proved for other polymers (McKee, Wilkes, Colby, & Long, 2004; Klossner, Queen, Coughlin, & Krause, 2008) that successful electrospinning only occurs at 2–2.5 times of the c_e. With increasing polymer concentration, the number of intermolecular associations between polymer chains was increased resulting in reduced fiber defects. However, the solution viscosity is also increased producing gels which show difficulties being spun via electrospinning. This was also the case with ulvan. Ulvan concentrations of 1.6% (w/v) and up to 3.2% (w/v) could form a visually homogenized gel. Yet, starting at 2.5% (w/v), a strong gelation occurred. From 4.8% (w/v) the material agglomerations were visible and up to 6.4% the dissolution was not possible (agglomerated parties). In an optimized ulvan gel, we have reached the ulvan concentration of 2.34% (w/v) by the aforementioned system (15 mM $B(OH)_3$; 7 mM $CaCl_2$: 60/40 (v/v)) at pH 6.9. This was the maximum amount of ulvan that produced an appropriate gel capable of performing electrospinning. Nevertheless, this gel was too viscous to be spinnable, leading to an electrospraying phenomenon.

Table 2
Fiber formation from ulvan/PVA mixed solutions.

Ulvan/PVA (solution mass ratio)[a]	Ulvan conc. (wt%)	PVA conc. (wt%)	Resulting polymer conc. (ulvan + PVA) (wt%)	Fiber diameter (nm)
50:50	1.2	6.0	7.2	105 ± 4
70:30	1.6	3.6	5.2	84 ± 4
85:15	2.0	1.8	3.8	60 ± 5

[a] Initial ulvan solutions were 2.34 wt% in 15 mM $B(OH)_3$; 7 mM $CaCl_2$: 60/40 and PVA solutions 12 wt% in deionized water.

An alternative path to achieve a successful electrospinning of ulvan was the introduction of a screening polymer such as PEO or PVA, in order to reduce the viscosity of the initial ulvan gel, making the gel spinnable at higher total polymer concentrations. In a first attempt, 3% (w/v) of PEO solutions were mixed with the 2.34% (w/v) solutions of ulvan. The mixed solutions were transparent, showing a good miscibility of the two polymers. When the PEO used was diluted in deionized water no electrospinning occurred, while with PEO diluted in 0.5 M acetic acid providing a dynamic viscosity of 560 mPa s, only bead defect nanofibers could be produced. The mixtures of ulvan/PEO (60:40) or ulvan/PEO (80:20) resulted in the same morphologically beaded structures (ESI, SF. 2). PEO as a nonionogenic flexible chain polymer is thought to interact with ulvan through hydrogen bonding. The oxygen atoms in the PEO backbone could contribute to the chain entanglement with ulvans intermolecular associations and facilitate the spinnability. Yet, either because the hydrogen associative forces are not strong enough in the case of ulvan, or because the total polymer content (up to 2.6% (w/v)) was not sufficient enough to lead to the appropriate chain entanglement, electrospinning could not generate defect-free nanofibers. Poly(vinyl alcohol) (PVA), a highly polar and biodegradable polymer can be electrospun easily. PVA is thought to provide better results than PEO, since it bears more hydroxyl groups in its backbone, capable to intercalate and better disrupt the ulvan's intermolecular interactions. Consequently, we have concentrated our attempts on the ulvan/PVA system.

3.2.1. Rheology of the ulvan/PVA solutions

The viscosity of polymer solutions is related to the intermolecular interactions among polymer chains. Ulvan is a highly charged polysaccharide. As the charge of the chain increases, the conformation of the chain in the solution expands and the viscosity increases. The gel formation of ulvan at a concentration of 1.6% (w/v) was reported (Lahaye & Axelos, 1993) to achieve a low elastic modulus (G') of about 3 Pa with boric acid alone which reached up to 250 Pa when $CaCl_2$ was added. In our experiments, it was also found that the storage modulus was greater than the loss modulus ($G' > G''$) at low frequencies, G' remaining constant for up to 8 Pa (see Fig. 2a); hence, this system is reported as viscoelastic gel. Both moduli are highly frequency-dependent and increase in a parallel manner at increasing frequency of oscillation. A crossover occurs at 29.2 Hz and only from that point on at higher frequencies, the loss modulus (G'') dominates G' (Fig. 2a).

When PVA was added to the ulvan's gel and mixed, G'' is dominating G' ($G'' > G'$) at low frequencies (Fig. 2b and c), which is typical for an entangled polysaccharide solution (Chronakis & Ramzi, 2002). The crossover frequency is observed at lower frequencies and has moved to decreased values of 11.1 Hz and 5.5 Hz accordingly, while the PVA content increased from 30% to 50% and the total polymer concentration from 5.2 wt% to 7.2 wt%, respectively (Table 2). This shift of the crossover point has been correlated (Chronakis & Ramzi, 2002) with the effective crosslinking change

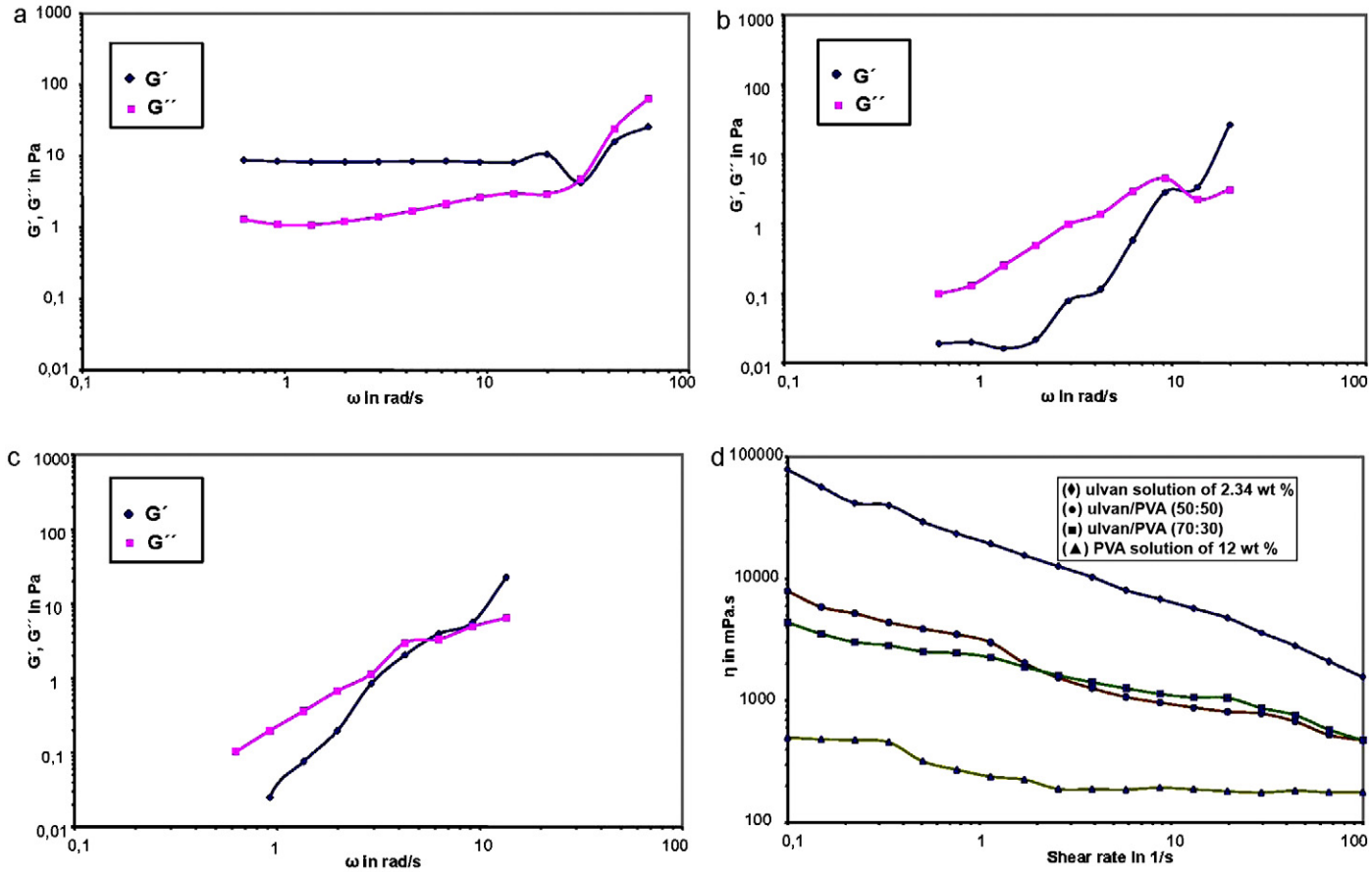

Fig. 2. Effect of total polymer concentration according to PVA addition in ulvan solution on storage (G') and loss (G'') moduli as function of frequency: (a) ulvan solution of 2.34 wt%, (b) 5.2 wt% ulvan/PVA (70:30) and (c) 7.2 wt% ulvan/PVA (50:50). In (d)shear viscosity of the above solutions as a function of shear rate: (♦) ulvan solution of 2.34 wt%, (●) ulvan/PVA (50:50), (■) ulvan/PVA (70:30) and (▲) PVA solution of 12 wt%.

or chain entanglement, thus with the higher electrospinning ability of a polymer solution (Nie et al., 2008).

In parallel, a net decrease in viscosity is observed with the addition of PVA. The initial dynamic viscosity of the 2.34% ulvan solution drops radically from 77,990 to 7922 mPa s for the ulvan/PVA (50/50) solution (see Fig. 2d). The decrease in viscosity with the addition of the co-blending polymer solution is due to inter and intra molecular interactions of ulvan chains. PVA can bind onto ulvan backbone disrupting the self-association of ulvan chains by a mechanism that is discussed in the following. The lower initial value observed for the ulvan/PVA (70/30) solution can be attributed to insufficient PVA binding according to fiber formation mechanism. This decrease in viscosity permits ulvan-based solutions to electrospin and allows nanofibers of progressively uniform morphology (see Fig. 4).

The decrease in elasticity which occurred within the ulvan/PVA system could also be correlated to a very high degree of alignment within the polymer, indicating a liquid crystal behavior similar to that observed in κ-carrageenan (Chronakis & Ramzi, 2002). Additionally, the differences between the oscillatory and the steady state shear characteristics are expressed by the simple application

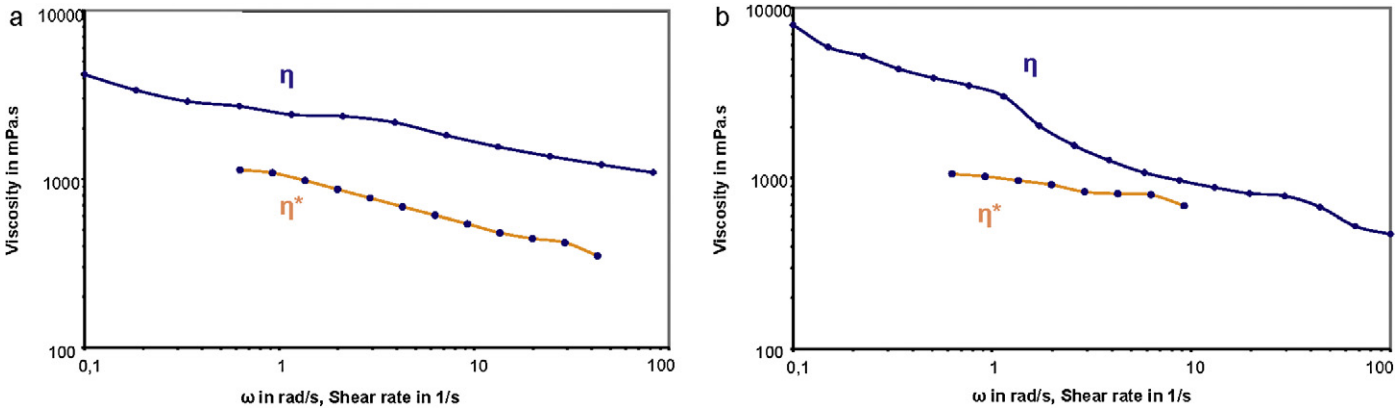

Fig. 3. Cox–Merz plot study of the (◊) steady shear viscosity η and (●) oscillatory or complex viscosity η^*: (a) ulvan/PVA (70:30) and (b) ulvan/PVA (50:50).

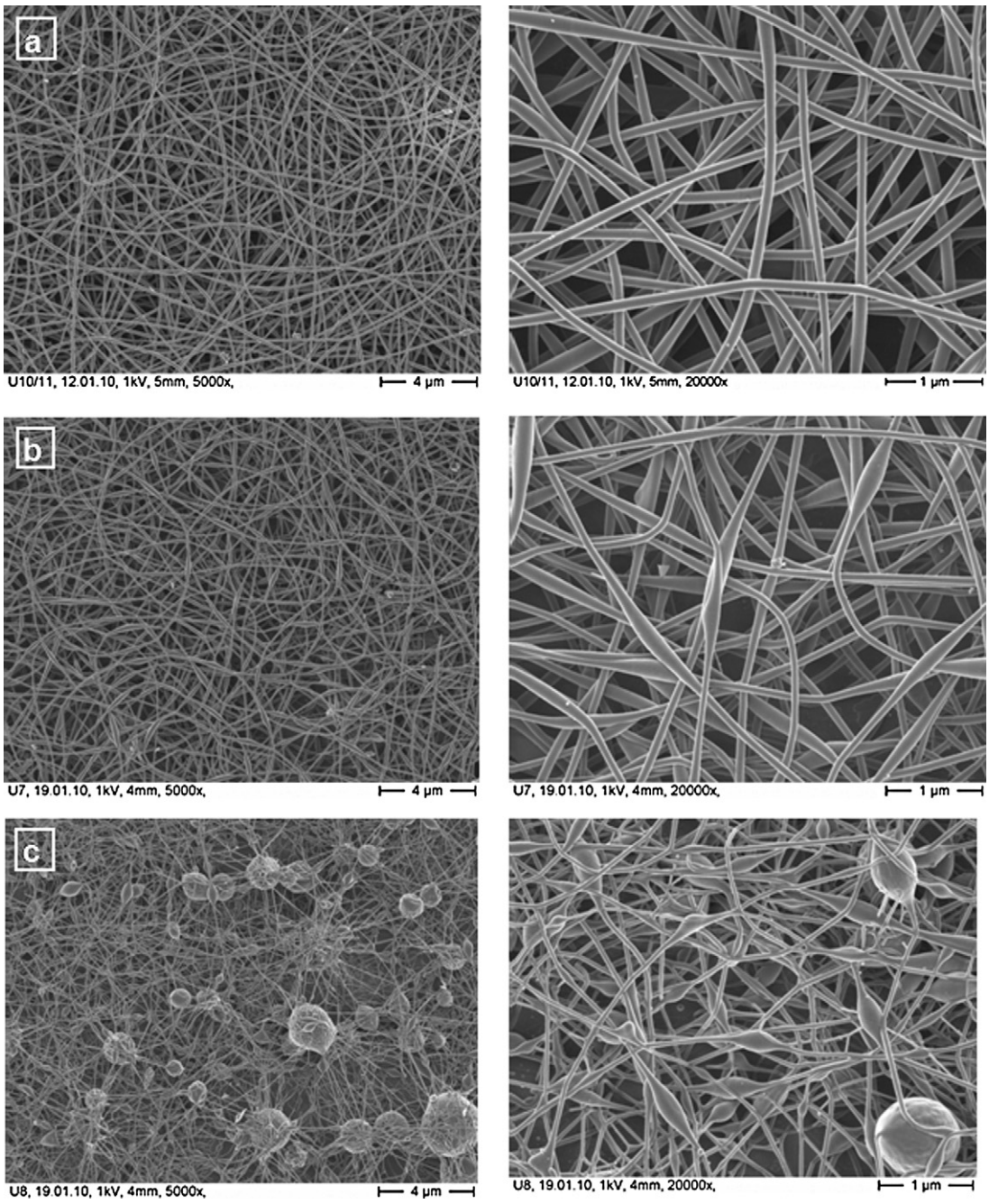

Fig. 4. SEM images of (a) ulvan/PVA (50:50) (top), (b) ulvan/PVA (70:30) (middle) and (c) ulvan/PVA (85:15) (bottom): effect of PVA content.

of the Cox–Merz rule. According to this rule, for ordinary polymers the complex viscosity (η^*) is coincided with the dynamic (η), for equal values of frequency of oscillation and shear rate. However, in case of liquid crystalline polymers, the steady-state values and the subsequent curve drop below (Chronakis & Ramzi, 2002) or ascend above the oscillatory values (Grizzuti, Moldenaers, Mortier, & Mewis, 1993). In our experiments, the steady shear viscosity curve is rising above the complex viscosity, thus deviating from the Cox–Merz rule and indicating the presence of shear-induced mesophase orientation (Fig. 3a and b). Therefore, ulvan which has been characterized as a thermoreversible gel (Lahaye & Robic, 2007) could eventually present an anisotropic phase with a chiral nematic structure (Borgström, Quist, & Piculell, 1996) as also evidenced by TEM (Fig. 5).

3.3. Nonwoven fabric from the ulvan/PVA blend system

The mixed ulvan/PVA solutions with respective ratios of 50/50 up to 70/30 resulted in defect-free electrospun nanofibers which have a very good uniformity (see Fig. 4).

The (50/50) ulvan/PVA solution provides perfectly uniform nanofibers with a diameter of 105 ± 4 nm. With the (70/30) ulvan/PVA solution, smaller nanofibers of 84 ± 4 nm were formed, presenting some thicker sections which can be attributed to the PVA non-uniform distribution. The central cross-sections (diameters) of these parts are approximately 177 ± 4 nm; this could refer to the observed PVA fibers with a mean diameter of 266 nm. In a higher ulvan ratio of (85/15) ulvan/PVA, in which the resulting polymer concentration is also reduced, greater beads of approx-

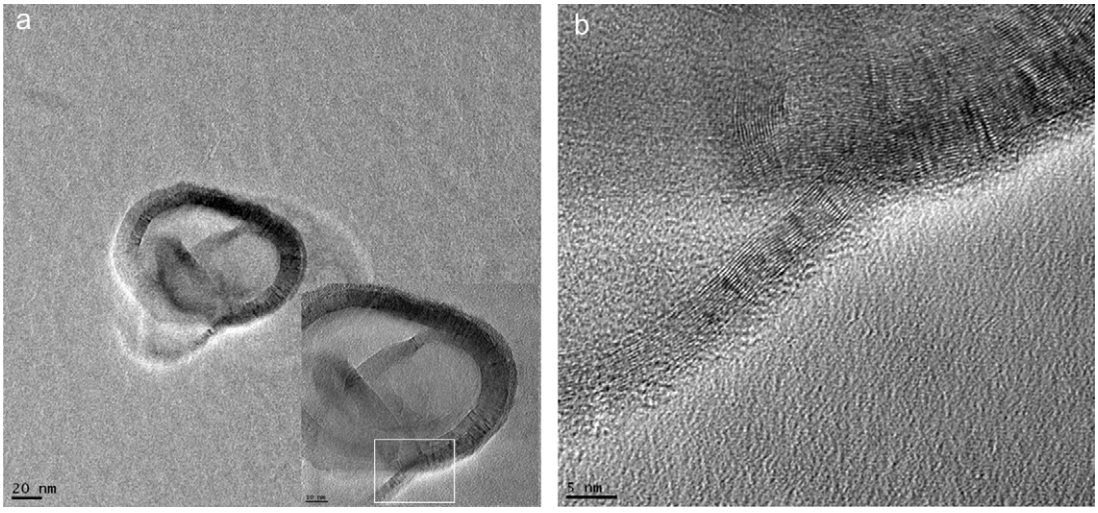

Fig. 5. TEM image of ulvan/PVA (50:50) nanofiber revealing the layered structure: the insight image in (a) and subsequently image (b) show part of a single nanofiber at higher magnification.

imately 1–2 μm together with smaller beads of 220 ± 8 nm are interconnected by thinner fibers of 60 ± 5 nm. These results show the gradual intercalation of PVA into the ulvan intermolecular or intramolecular structures, dependent on the PVA ratio. In general, fiber diameters decrease with increasing ulvan concentration and bead formations decrease as total polymer concentration (ulvan + PVA) increase (Table 2).

The solutions showed slight degradation when re-injected after 20 days, as evidenced by the formation of nanofibrils (ESI, SF. 3); this result being in favor of a complex fiber formation. The electrospun fibers were soluble when immersed for 48 h in DMEM (Dulbecco's Modified Eagle's Medium). For applications in which the mechanical integrity is critical, this should impose a chemical cross-linking for example with the natural extract genipin (Hillberg, Holmes, & Tabrizian, 2009). But for applications such as the controlled release of substances, the degradability of the material can be acceptable and desirable.

3.3.1. Transmission electron microscopy

The examination of single ulvan/PVA nanofiber (Fig. 5a) with the high resolution transmission electron microscopy (HRTEM) shows not only a layered structure but quite interestingly also reveals a highly ordered structure (see Fig. 5b).

The HRTEM images clearly show that the ulvan/PVA nanofibers present multiple shells of 14 layers in their crystalline structure, and a shell *d*-spacing of about 0.36 nm. A similar high degree of order has been observed on nanocomposite fibrils containing single wall carbon nanotubes (SWNTs) (Ko et al., 2003), on carbon nitride (CN*x*) nanotubes (Ghosh, Kumar, Maruyama, & Ando, 2010) and TiO_2 nanofibers (Yuan & Su, 2004). On the contrary, the pure PVA fibers normally possess smooth surfaces (Cho, Kim, Choi, Kim, & Kim, 2010). Although the crystallization has been noticed to be retarded due to electrospinning (Liu, Wu, & Reneker, 2000; Zong et al., 2002), these results point out the presence of regular sequences of ulvan; and this, in spite of the fact that they can also perform an order–disorder conformational transition dependent on the iduronic ring equilibrium conformation (Paradossi et al., 2002). It should also be noticed that many semirigid macromolecules can form both gels and liquid crystalline ordered phases such as nematic or chiral nematic (Chronakis & Ramzi, 2002), and this has been observed in many other natural polysaccharides, such as chitin or xanthan as well. Nevertheless, further investigations are needed in order to prove the presence of long-range liquid crystalline order in aqueous solution.

3.4. Formation of complex ulvan/PVA nanofibers

Ulvan is a lightly branched anionic polysaccharide containing two negatively charged groups, carboxylates and sulfate esters in the repeating disaccharides consisting of glucuronic or iduronic acid and rhamnose sulfate. Also, as it was observed with other cationic polysaccharides, repulsive interaction among the polyanions should prevent sufficient chain entanglement (Li & Hsieh, 2006) necessary for fiber formation. However, the ulvan gel formation has the unique characteristic of involving borate esters (Haug, 1976). The mechanism of gel formation is not yet completely unveiled. Boric acid and borate are in equilibrium in solution and borate ions can form esters with 1,2-diols (Henderson, How, Kennedy, & Mooney, 1973) which have been proposed to cross-link ulvan via Ca (II) ions stabilization (Haug, 1976; Lahaye & Axelos, 1993). And recently it was clarified that the ulvan's gel formation occurs as an aggregate of spherical-shaped structures interconnected with filament-like material, involving similar ionic interactions (Robic, Gaillard, et al., 2009).

In our experiments, PEO is considered to intercalate within the ulvan chains, forming hydrogen bonds (see Scheme 1a). On the contrary, PVA could interpenetrate inside the ulvan aggregates or chains and form a stabilized polyelectrolyte complex, resulting in uniform fibers. In this case, the unlike structure proposed by Haug (Haug, 1976) for the direct ulvan cross-link by borate esters mediated by Ca (II) cations, could apply. Thus, direct cross-links via the exposed PVA hydroxyl groups could interconnect PVA with ulvan via the borate esters resulting in a stronger assembly (see Scheme 1b). This argument is supported by the interaction between PVA and boric acid in aqueous medium known for a long time, leading to poly(vinyl borate) (PVBO) ester formation (Chetri, Dass, & Sarma, 2007; Marvel & Denoon, 1938; Shibayama, Hiroyouki, Hidenobu, Hiroshi, & Shunji, 1988; Thiele & Lamp, 1960). When the PVA solution is added and mixed with the ulvan-borate gel, the still free borate hydroxyl groups which are weakly stabilized by the calcium ions could further react with PVA's exposed hydroxyls and link the ulvan to PVA chains via post-esterification.

Therefore, increasing the PVA content ratio up to an equal ratio of ulvan and PVA, significantly improved the uniformity and

formation efficiency of the complex nanofibers. On the other hand, the beaded fibers (see Fig. 4c, bottom) obtained with the lower PVA content, ulvan/PVA (85/15), argue for the ulvan's gel formation structure proposed by Robic, Gaillard, et al. (2009).

3.5. Composition of the electrospun ulvan/PVA fibers

The ulvan/PVA blended nanofibers present an integrated structure without component partitioning or porous structures, suggesting good "miscibility". The SEM images (ESI, SF. 4) are also supporting the new ulvan/PVA complex nanofiber formation. It has generally been postulated in electrospinning (Chakraborty, Liao, Adler, & Leong, 2009; Zhang, Su, Ramakrishna, & Lim, 2008) that the fibers' diameters reduce by increasing the distance between the needle and the collector. However, this was not observed with PVA (Zhang, Yuan, Wu, & Sheng, 2005). On the contrary, this was observed in our experiments, not only for PVA nanofibers electrospun from a 12% PVA solution but also for the ulvan/PVA (50:50) nanofibers electrospun under the same conditions. The operating parameters in this study were specific: 20–25 kV of applied voltage for the PVA, and 28 kV for the ulvan/PVA blends, 0.04 mL/h solution feeding rate, and ambient conditions of 33% humidity and 22 °C temperature with the critical distances for the solutions being 7 and 12 cm, respectively. The PVA solution formed nanofibers with a mean diameter of 328 nm at a distance of 7 cm decreasing to 266 nm when spun at 12 cm from the collector. That means that the PVA fiber diameters are reduced by 1.2 times. The ulvan/PVA (50:50) solutions produce corresponding nanofibers of 150 nm at 7 cm, shortening to a mean diameter of 105 nm at 12 cm of tip-to-collector distance (ESI, SF. 4). In this case, the fiber diameters' reduction is calculated at 1.4 times. Yet, more important is the decrease in fiber diameter observed between ulvan/PVA and pure PVA. At a distance of 7 cm, the ulvan/PVA nanofibers have 2.2 times finer diameters than the PVA nanofibers while, when the distance is 12 cm, the ulvan/PVA nanofibers are 2.5 times thinner than the PVA ones. This late remark opts also for the formation of new complex ulvan/PVA nanofibers and accounts for the ulvan's ability to form polyelectrolyte fibers. In fact, the contracting fiber effect upon the addition of PVA could also be interpreted as originated from the stronger ionic complex formed between ulvan and PVA, involving hydroxyl groups and borate esters as described in Scheme 1b.

This was supported by the infrared (IR) spectroscopy experiments. The two spectra of ulvan in Fig. 6A and B, are recorded from a raw material sample and a solution of 2.34% ulvan in H_3BO_3–$CaCl_2$, respectively, prepared as reported in the experimental section and used in electrospinning. Even if ulvan is shown to maintain its structure in solution, a difference in the spectrum of ulvan's solution is observed within the wavelengths between 980 and 1050 cm^{-1}. This could be attributed to the B–OH and B–O groups of the boric acid (Chetri et al., 2007).

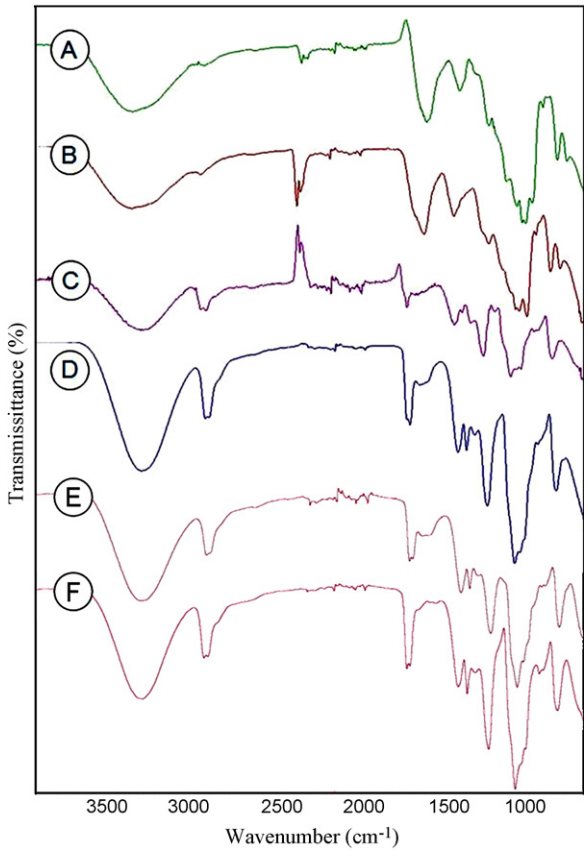

Fig. 6. IR spectra of (A) ulvan extract from *Ulva rigida*, (B) 2.34% ulvan solution, (C) solution of ulvan/PVA (50:50), (D) electrospun ulvan/PVA (50:50), (E) electrospun ulvan/PVA (70:30), and (F) 12% PVA solution.

The IR spectrum of PVA depicts characteristic absorption bands at 3330, 2940, 1733, 1428, 1374, 1247, 1091 and 838 cm^{-1}, which are attributed to the ν (OH), ν_α (CH_2), ν (C=O), δ (CH_2), γ_ω (CH_2), γ_ω (CH), ν (C–O) and ν (C–C) resonances, respectively (Krimm, Liang, & Sutherland, 1956; Li & Hsieh, 2006). A smaller band (see Fig. 6F) at 1322 cm^{-1} is characteristic of the δ (CH–OH) assignment (Krimm et al., 1956; Zheng, Du, Yu, Huang, & Zhang, 2001).

The spectrum in Fig. 6C shows the absorptions of the ulvan/PVA (50:50) solution. We observe the net amplification of the peak corresponding to sulfate ester (C–O–S) of ulvan's rhamnose at 1248 cm^{-1} and the simultaneous growth of the ν_α (CH_2) assignment at 2911–2940 cm^{-1} from the PVA. The same observations are

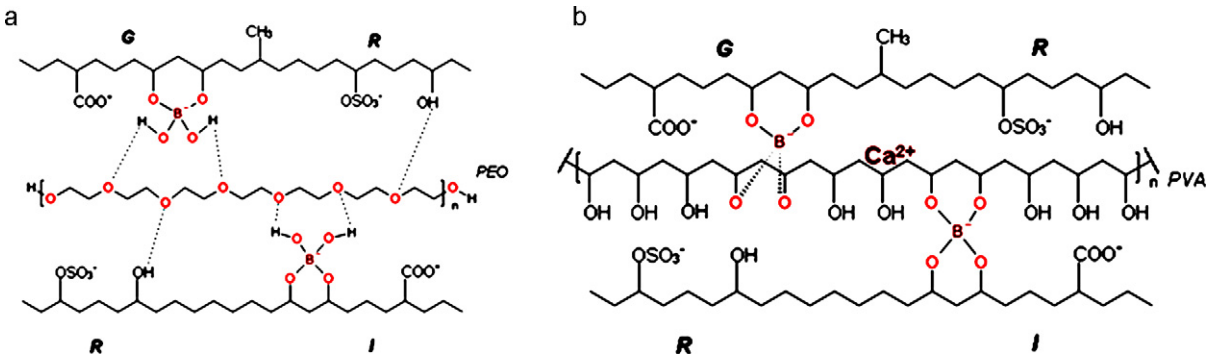

Scheme 1. Schematic representation of ulvan-based complex fiber formation upon a random disaccharide configuration. (a) Intercalation of PEO via hydrogen bonds. (b) Interaction of PVA with ulvan via hydroxyl groups involving borate esters: stabilized ionic polyelectrolyte fiber.

deducted for the spectrum of the electrospun ulvan/ PVA (50:50) nanofibers (see Fig. 6D). We remark a further enhancement of the bands at 1249 cm^{-1} (C–O–S) and 2911–2940 cm^{-1} (CH_2) and a net increase of the peaks at 3320, 1713 and 1087 cm^{-1} characteristic to the (OH) and (–COO) carboxylate groups of the uronic acids. At the same time the absorption peak concerned with –OH stretching vibrations has shifted to lower wave number while the peak corresponding to the carboxylate groups has shifted from 1620 cm^{-1} to a higher wave number of 1713 cm^{-1}. Finally, at the spectrum of electrospun ulvan/PVA (70:30) blend (Fig. 6E), we clearly note the formation of a double peak at 1615 and 1652 cm^{-1} of (–COO) near the PVA's ν (C=O) assignment at 1733 cm^{-1} in comparison to the PVA spectrum (Fig. 6F). However, the assignment at 1600 cm^{-1} (see Fig. 6D and E) has also been attributed to the cyclic borate ester (Chetri et al., 2007). Also, the band at 1060 cm^{-1} accentuated in the spectrum of ulvan/PVA (50/50) nanofibers is characteristic to the B–O group, indicating the borate involvement in the fiber formation.

The results of IR measurements indicate the formation of new resonances that cannot be accounted for a simple mixture. All of the above examined remarks of the spectra comparison are consistent with a new complex formation.

4. Conclusion

Uniform ulvan-based nanofibers blended with PVA, having a very narrow diameter distribution controllable down to 84 nm were fabricated by electrospinning. The nanofibers were deposited as a nonwoven membrane without interconnections and presented a high degree of orientation, attributed to the ulvan component. Rheological study combined with SEM characterization revealed that the spinnability of ulvan-based solution was substantially improved when the solution viscosity was reduced. The fibers presented a highly ordered structure under TEM probably due to mesophase formation promoted by the Cox–Merz rule, while the IR results suggested a good integration of the PVA chains into the ulvan. The possible interpenetration mechanisms related to rheological data were discussed for PEO and PVA. A new fiber is considered to be created upon the addition of PVA to ulvan, resulting from ionic assembly in the presence of borate esters and divalent cations. Additional studies are needed in order to clarify the chain's expansion mode and the complex viscoelastic behavior of ulvan. The possibility to electrospin pure ulvan in higher concentrations should then be further examined. The mechanical properties, cytotoxicity of the system and comparison with other natural polysaccharides are currently under investigation in order to elucidate the potentialities of this new material.

However, the fiber ability of this anionic polyelectrolyte could greatly contribute to the knowledge of its properties still unrevealed. This fibrous material presents characteristics which could positively combine in specific domains: it dissolves poorly in water and as dietary fiber is not degraded by human digestive enzymes, the anticoagulant, antioxidant and antithrombotic activities of this sulfated polysaccharide, related to its proven spinnability could lead to new biomedical applications. These could include drug delivery, wound dressing applications as well as the tissue engineering field, if mechanical integrity was reinforced. The possible combination of this anionic polysaccharide fiber with other biomaterials can extend the aforementioned application areas. Finally, the biocompatibility and bioactivity of this promising biopolymer could unveil a potential biomaterial from cheap natural resources.

Acknowledgements

This research was funded by the SFB 528 Project, Germany. The authors thank Mrs. Ortrud Trommer and Marianne Reibold for their invaluable help with SEM and TEM, respectively; also Petros Katapodis of the National Technical University of Athens, School of Chemical Engineering, Division IV – Product and Process Development, Laboratory of Biotechnology and Laboratory of Food Chemistry and Technology, and Mr. Ramzi Chaouch for the technical assistance.

Appendix A. Supplementary data

Supplementary data associated with this article can be found, in the online version, at doi:10.1016/j.carbpol.2010.12.075

References

Blumenkrantz, N., & Asboe-Hansen, G. (1973). New method for quantitative determination of uronic acids. *Analytical Biochemistry*, *54*, 484–489.
Borgström, J., Quist, P. O., & Piculell, L. (1996). A novel chiral nematic phase in aqueous kappa-carrageenan. *Macromolecules*, *29*, 5926–5933.
Chakraborty, S., Liao, I. C., Adler, A., & Leong, K. W. (2009). Electrohydrodynamics: A facile technique to fabricate drug delivery systems. *Advanced Drug Delivery Reviews*, *61*, 1043–1054.
Chetri, P., Dass, N. N., & Sarma, N. S. (2007). Conductivity measurement of poly(vinyl borate) and its lithium derivative in solid state. *Materials Science and Engineering: B*, *139*, 261–264.
Chiellini, E., Cinelli, P., Ilieva, V. I., & Martera, M. (2008). Biodegradable thermoplastic composites based on polyvinyl alcohol and algae. *Biomacromolecules*, *9*, 1007–1013.
Cho, K., Kim, M., Choi, K. M., Kim, K., & Kim, S. (2010). Synthesis and characterization of electrospun polymer nanofibers incorporated with CdTe nanoparticles. *Synthetic Metals*, *160*, 888–891.
Chronakis, I. S., & Ramzi, M. (2002). Isotropic-nematic phase equilibrium and phase separation of κ-carrageenan in aqueous salt solution: Experimental and theoretical approaches. *Biomacromolecules*, *3*, 793–804.
Chupa, J. M., Foster, A. M., Sumner, S. R., Madihally, S. V., & Matthew, H. W. (2000). Vascular cell responses to polysaccharide materials: In vitro and in vivo evaluations. *Biomaterials*, *21*, 2315–2322.
Dubois, M. K., Gilles, A., Hamilton, J. K., Rebers, P. A., & Smith, F. (1956). Colorimetric method for determination of sugars and related substances. *Analytical Chemistry*, *28*, 350–356.
Ghosh, K., Kumar, M., Maruyama, T., & Ando, Y. (2010). Controllable growth of highly N-doped carbon nanotubes from imidazole: A structural, spectroscopic and field emission study. *Journal of Materials Chemistry*, *20*, 4128–4134.
Graessley, W. W. (1980). Polymer chain dimensions and the dependence of viscoelastic properties on concentration, molecular weight and solvent power. *Polymer*, *21*, 258–262.
Greiner, A., & Wendorf, J. H. (2007). Electrospinning: A fascinating method for the preparation of ultrathin fibers. *Angewandte Chemie International Edition*, *46*, 5670–5703.
Grizzuti, N., Moldenaers, P., Mortier, M., & Mewis, J. (1993). On the time-dependency of the flow-induced dynamic moduli of a liquid crystalline hydroxypropylcellulose solution. *Rheologica Acta*, *32*, 218–226.
Haug, A. (1976). The influence of borate and calcium on the gel formation of a sulfated polysaccharide from Ulva lactusa. *Acta Chemica Scandinavica*, *B30*, 562–566.
Henderson, W. G., How, M. J., Kennedy, G. R., & Mooney, E. F. (1973). The interconversion of aqueous boron species and the interaction of borate with diols: A ^{11}B NMR study. *Carbohydrate Research*, *28*, 1–12.
Hillberg, A. L., Holmes, C. A., & Tabrizian, M. (2009). Effect of genipin cross-linking on the cellular adhesion properties of layer-by-layer assembled. *Polyelectrolyte Films Biomaterials*, *30*, 4463–4470.
Jagur-Grodzinski, J. (2006). Polymers for tissue engineering, medical devices and regenerative medicine. Concise general review of recent studies. *Polymers for Advanced Technologies*, *17*, 395–418.
Jiang, H., Fang, D., Hsiao, B. S., Chu, B., & Chen, W. (2004). Optimization and characterization of dextran membranes prepared by electrospinning. *Biomacromolecules*, *5*, 326–333.
Kaeffer, B., Benard, C., Lahaye, M., Blottiere, H. M., & Cherbut, C. (1999). Biological properties of ulvan, a new source of green seaweed sulfated polysaccharides, on cultured normal and cancerous colonic epithelial cells. *Planta Medica*, *65*, 527–531.
Kawai, Y., Seno, N., & Anno, K. (1969). A modified method for chondrosulfatase assay. *Analytical Biochemistry*, *32*, 314–321.
Klossner, R. R., Queen, H. A., Coughlin, A. J., & Krause, W. E. (2008). Correlation of chitosan's rheological properties and its ability to electrospin. *Biomacromolecules*, *9*, 2947–2953.
Ko, F., Gogotsi, Y., Ali, A., Naguib, N., Ye, H., Yang, G., & Willis, P. (2003). Electrospinning of continuous carbon nanotube-filled nanofiber yarns. *Advanced Materials*, *15*, 1161–1165.
Krimm, S., Liang, C. Y., & Sutherland, G. B. B. M. (1956). Infrared spectra of high polymers. V. Polyvinyl alcohol. *Journal of Polymer Science*, *22*, 227–247.
Lahaye, M. (1998). NMR spectroscopic characterization of oligosaccharides from two Ulva rigida ulvan samples (Ulvales Chlorophyta) degraded by a lyase. *Carbohydrate Research*, *314*, 1–12.

Lahaye, M., & Axelos, M. A. V. (1993). Gelling properties of water-soluble polysaccharides from proliferating marine green seaweeds (Ulva spp.). *Carbohydrate Polymers*, *22*, 261–265.
Lahaye, M., & Kaeffer, B. (1997). Seaweed dietary fibers structure physicochemical and biological properties relevant to intestinal physiology. *Sciences des Aliments*, *17*, 563–584.
Lahaye, M., & Ray, B. (1996). Cell-wall polysaccharides from the marine green alga Ulva "rigida" (Ulvales Chlorophyta) – NMR analysis of ulvan oligosaccharides. *Carbohydrate Research*, *283*, 161–173.
Lahaye, M., & Robic, A. (2007). Structure and functional properties of ulvan, a polysaccharide from green seaweeds. *Biomacromolecules*, *8*, 1765–1774.
Lahaye, M., Alvarez-Cabal Cimadevilla, E., Kuhlenkamp, R., Quemener, B., Lognoné, V., & Dion, P. (1999). Chemical composition and ^{13}C NMR spectroscopic characterisation of ulvans from Ulva (Ulvales, Chlorophyta). *Journal of Applied Psychology*, *11*, 1–7.
Lahaye, M., Brunel, M., & Bonnin, E. (1997). Fine chemical structure analysis of oligosaccharides produced by an ulvan-lyase degradation of the water-soluble cell-wall polysaccharides from Ulva sp. (Ulvales Chlorophyta). *Carbohydrate Research*, *304*, 325–333.
Lahaye, M., Inizan, F., & Vigouroux, J. (1998). NMR analysis of the chemical structure of ulvan and of ulvan–boron complex formation. *Carbohydrate Polymers*, *36*, 239–249.
Lee, K. Y., Jeong, L., Kang, Y. O., Lee, S. J., & Park, W. H. (2009). Electrospinning of polysaccharides for regenerative medicine. *Advanced Drug Delivery Reviews*, *61*, 1020–1032.
Li, L., & Hsieh, Y. L. (2006). Chitosan bicomponent nanofibers and nanoporous fibers. *Carbohydrate Research*, *341*, 374–381.
Liu, W., Wu, Z., & Reneker, D. H. (2000). Structure and morphology of poly(metaphenylene isophthalamide) nanofibers produced by electrospinning. *Polymer Preprints*, *41*, 1193–1194.
Mano, J. F., & Reis, R. L. J. (2007). Osteochondral defects: Present situation and tissue engineering approaches. *Journal of Tissue Engineering and Regenerative Medicine*, *1*, 261–273.
Mao, W., Zang, X., Li, Y., & Zhang, H. (2006). Sulfated polysaccharides from marine green algae Ulva conglobata and their anticoagulant activity. *Journal of Applied Psychology*, *18*, 9–14.
Marvel, C. S., & Denoon, C. E. (1938). Structure of vinyl polymers II. Polyvinyl alcohol. *Journal of the American Chemical Society*, *60*, 1045–1051.
McKee, M. G., Wilkes, G. L., Colby, R. H., & Long, T. E. (2004). Correlations of solution rheology with electrospun fiber formation of linear and branched polyesters. *Macromolecules*, *37*, 1760–1767.
Morelli, A., & Chiellini, F. (2010). Ulvan as a new type of biomaterial from renewable resources: Functionalization and hydrogel preparation. *Macromolecular Chemistry and Physics*, *211*, 821–832.
Nie, H., He, A., Zheng, J., Xu, S., Li, J., & Han, C. C. (2008). Effects of chain conformation and entanglement of pure alginate. *Biomacromolecules*, *9*, 1362–1365.
Paradossi, G., Cavalieri, F., & Chiessi, E. (2002). A conformational study on the algal polysaccharide ulvan. *Macromolecules*, *35*, 6404–6411.
Paradossi, G., Cavalieri, F., Pizzoferrato, L., & Liquori, A. M. (1999). A physico-chemical study on the polysaccharide ulvan from hot water extraction of the macroalga Ulva. *International Journal of Biological Macromolecules*, *25*, 309–315.
Pengzhan, Y., Quanbin, Z., Ning, L., Zuhong, X., Yanmei, W., & Zhi'en, L. (2003). Polysaccharides from Ulva pertusa (Chlorophyta) and preliminary studies on their antihyperlipidemia activity. *Journal of Applied Psychology*, *15*, 21–27.
Qi, H., Zhang, Q., Zhao, T., Hu, R., Zhang, K., & Li, Z. (2006). In vitro antioxidant activity of acetylated and benzoylated derivatives of polysaccharide extracted from Ulva pertusa (Chlorophyta). *Bioorganic Medicinal Chemistry Letters*, *16*, 2441–2445.
Qi, H., Zhao, T., Zhang, Q., Li, Z., Zhao, Z., & Xing, R. (2005). Antioxidant activity of different molecular weight sulfated polysaccharides from Ulva pertusa Kjellm (Chlorophyta). *Journal of Applied Psychology*, *17*, 527–534.
Quemener, B., Lahaye, M., & Bobin Dubigeon, C. J. (1997). Sugar determination in ulvans by a chemical-enzymatic method coupled to high performance anion exchange chromatography. *Journal of Applied Psychology*, *9*, 179–188.
Quemener, B., & Thibault, J. F. (1990). Assessment of methanolysis for the determination of sugars in pectins. *Carbohydrate Research*, *206*, 277–287.
Ray, B., & Lahaye, M. (1995). Cell-wall polysaccharides from the marine green alga Ulva "rigida" (Ulvales Chlorophyta). Chemical structure of ulvan. *Carbohydrate Research*, *274*, 313–318.
Reneker, D. H., Yarin, A. L., Fong, H., & Koombhongse, S. (2000). Bending instability of electrically charged liquid jets of polymer solutions in electrospinning. *Journal of Applied Physics*, *87*, 4531–4547.
Robic, A., Bertrand, D., Sassi, J. F., Lerat, Y., & Lahaye, M. (2009). Determination of the chemical composition of ulvan, a cell wall polysaccharide from Ulva spp. (Ulvales Chlorophyta) by FT-IR and chemometrics. *Journal of Applied Psychology*, *21*, 451–456.
Robic, A., Gaillard, C., Sassi, J. F., Lerat, Y., & Lahaye, M. (2009). Ultrastructure of Ulvan: A polysaccharide from green seaweeds. *Biopolymers*, *91*, 652–664.
Robic, A., Rondeau-Mouro, C., Sassi, J. F., Lerat, Y., & Lahaye, M. (2009). Structure and interactions of ulvan in the cell wall of the marine green algae Ulva rotundata (Ulvales Chlorophyceae). *Carbohydrate Polymers*, *77*, 206–216.
Sassaki, G. L., Souza, L. M., Serrato, R. V., Cipriani, T. R., Gorin, P. A. J., & Iacomini, M. (2008). Application of acetate derivatives for gas chromatography–mass spectrometry: Novel approaches on carbohydrates, lipids and amino acids analysis. *Journal of Chromatography A*, *1208*, 215–222.
Shibayama, M., Hiroyouki, Y., Hidenobu, K., Hiroshi, F., & Shunji, N. (1988). Sol–gel transition of poly(vinyl alcohol)–borate complex. *Polymer*, *29*, 2066–2071.
Stevens, M. M. (2008). Biomaterials for bone tissue engineering. *Materials Today*, *11*, 18–25.
Taboada, C., Millán, R., & Míguez, I. (2010). Composition, nutritional aspects and effect on serum parameters of marine algae Ulva rigida. *Journal of the Science of Food and Agriculture*, *90*, 445–449.
Thiele, H., & Lamp, H. (1960). Über die Spinnbarkeit kolloider Systeme. *Colloid and Polymer Science*, *173*, 63–72.
Toskas, G., Laourine, E., Kaeosombon, W., & Cherif, C. (2009). Electrospinning of collagen and chitosan in perspective of medical scaffolds applications. In *International conference on latest advancements in high tech textiles and textile-based materials* Gent, Belgium,
Venugopal, S., & Ramakrishna, S. (2005). Applications of polymer nanofibers in biomedicine and biotechnology. *Applied Biochemistry and Biotechnology*, *125*, 147–157.
Webster, E. A., Murphy, A. J., Chudek, J. A., & Gadd, G. M. (1997). Metabolism-independent binding of toxic metals by Ulva lactuca: Cadmium binds to oxygen-containing groups, as determined by NMR. *BioMetals*, *10*, 105–117.
Yu, P., Li, N., Liu, X., Zhou, G., Zhang, Q., & Li, P. (2003). Antihyperlipidemic effects of different molecular weight sulfated polysaccharides from Ulva pertusa (Chlorophyta). *Pharmacological Research*, *48*, 543–549.
Yuan, Z. Y., & Su, B. L. (2004). Titanium oxide nanotubes, nanofibers and nanowires. *Colloids and Surfaces A: Physicochemical and Engineering Aspects*, *241*, 173–183.
Zhang, C., Yuan, X., Wu, L., & Sheng, J. (2005). Study of electrospun poly(vinyl alcohol) mats. *European Polymer Journal*, *41*, 423–432.
Zhang, H. J., Mao, W. J., Fang, F., Li, H. Y., Sun, H. H., Ghen, Y., & Qi, X. H. (2008). Chemical characteristics and anticoagulant activities of a sulfated polysaccharide and its fragments from Monostroma latissimum. *Carbohydrate Polymers*, *71*, 428–434.
Zhang, Y. Z., Su, B., Ramakrishna, S., & Lim, C. T. (2008). Chitosan nanofibers from an easily electrospinnable UHMWPEO-doped chitosan solution system. *Biomacromolecules*, *9*, 136–141.
Zheng, H., Du, Y., Yu, J., Huang, R., & Zhang, L. (2001). Preparation and characterization of chitosan/poly(vinyl alcohol) blend fibers. *Journal of Applied Polymer Science*, *80*, 2558–2565.
Zong, X., Kim, K., Fang, D., Ran, S., Hsiao, B. S., & Chu, B. (2002). Structure and process relationship of electrospun bioabsorbable nanofiber membranes. *Polymer*, *43*, 4403–4412.